Biosensors and Bioelectronics 124–125 (2019) 199–204

Contents lists available at ScienceDirect

Biosensors and Bioelectronics

journal homepage: www.elsevier.com/locate/bios

Simultaneous detection of telomerase and miRNA with graphene oxide-based fluorescent aptasensor in living cells and tissue samples

Xiaowen Ou[a,1], Shenshan Zhan[a,1], Chunli Sun[a], Yong Cheng[a,*], Xudong Wang[a], Bifeng Liu[a], Tianyou Zhai[a], Xiaoding Lou[b], Fan Xia[a,b]

[a] State Key Laboratory of Material Processing and Die & Mould Technology, School of Materials Science and Engineering, Hubei Key Laboratory of Bioinorganic Chemistry & Materia Medica, School of Chemistry and Chemical Engineering, National Engineering Research Center for Nanomedicine, Department of Biomedical Engineering, College of Life Science and Technology, Huazhong University of Science and Technology, Wuhan 430074, PR China

[b] Engineering Research Center of Nano-Geomaterials of Ministry of Education, Faculty of Materials Science and Chemistry, China University of Geosciences, Wuhan 430074, PR China

ARTICLE INFO

Keywords:
Simultaneous detection
Graphene oxide
Fluorescent aptasensor
Telomerase
MiRNA

ABSTRACT

Telomerase and microRNAs (miRNAs) as important biomarkers are closely related to cancers. Simultaneous detection of telomerase activity and miRNAs would be beneficial to improve the specificity and reliability. Here, we establish a telomerase and miRNA-21 (miR-21) simultaneous sensing platform with graphene oxide-based fluorescent aptasensors (GOFA) including graphene oxide (GO), template strand (TS) primer and fluorophore-labeled telomerase/miR-21 oligonucleotides. Owing to π-π stacking interaction, TS primer and telomerase/miR-21 probes would be loaded onto GO, resulting in fluorescence quenching. However, in the presence of the telomerase or miR-21, the double-stranded oligonucleotides would be away from the GO surface attribute to the hybridization between the extended TS primers and telomerase probe as well as miR-21 and miR-21 probe, leading to obvious fluorescence recovery. We found that GOFA could simultaneously detect telomerase activity and miR-21 with low background signal, high sensitivity and simplified operation. Moreover, GOFA could be used for accurately detecting telomerase activity and miRNA in living cells and cancer patient tissue sample. This sensing platform shows great potential in improving the accuracy in clinical diagnosis of cancer.

1. Introduction

The aberrant expressed biomarkers in certain patients are closely associated with cancers. The detection of biomarkers with high sensitivity and selectivity is essential for cancer prevention, diagnosis and therapy as well as the understanding of cancer pathogenesis (Cheng et al., 2018; Wu and Qu, 2015; Etzioni et al., 2003). Consequently, to improve the specificity and reliability of multi-targets detection as a major issue has been aroused wide attention. Telomerase as one of the most representative biomarkers could add specific sequence $(AATCCG)_n$ to telomere using its template RNA after combining with template strand (TS) primer. Moreover, it has been testified that telomerase is over-expressed in more than 85% human tumors but not in normal cells (Lou et al., 2015; Zhou and Xing, 2012; Blasco, 2005). On the other hand, some special microRNAs (miRNAs) are another kinds of important biomarkers including a series of small noncoding RNAs with the length of 18–25 nt. It has been found that the abnormal expression of miRNAs have been linked to the cancers (Wang et al., 2018; Croce, 2009). So far, various strategies have been reported for telomerase activity and miRNA analysis (Pan et al., 2018; Wei et al., 2018; Yang et al., 2018; Pan et al., 2013; Li et al., 2012), such as the polymerase chain reaction (PCR)-based classic telomeric repeat amplification and the nanomaterial-based sensing platform (Long et al., 2018; Qian et al., 2014; Du et al., 2012; Agasti et al., 2010). Among these methods, isothermal enzymatic amplification has attracted much attention due to its simple operation and high sensitivity (Zhang et al., 2017a, 2017b, 2017c; Zhao et al., 2015; Duan et al., 2013). However, the fluorescent signals from background noise of intact probes always affect the sensitivity of detection. Therefore, there is an urgent desired to establish a versatile system for the efficient and multi-targets simultaneous detection.

It is well known that graphene oxide (GO) not only could absorb

* Correspondence to: State Key Laboratory of Material Processing and Die & Mould Technology, School of Materials Science and Engineering, Huazhong University of Science and Technology, Wuhan 430074, PR China.
E-mail address: chengy@hust.edu.cn (Y. Cheng).
[1] These authors contributed equally to this work.

https://doi.org/10.1016/j.bios.2018.10.009
Received 21 July 2018; Received in revised form 18 September 2018; Accepted 4 October 2018
Available online 17 October 2018
0956-5663/

single-stranded DNA (ssDNA) through π-π stacking interaction and quench the fluorescence of fluorophore-labeled ssDNA (Pei et al., 2012; Liu et al., 2010; Loh et al., 2010), but also shows good biocompatibility, efficient intracellular transport capacity and protection for nucleic acids from enzymatic cleavage (Zang et al., 2017; Zhang et al., 2017a, 2017b, 2017c; Wang et al., 2013). Therefore, GO has been widely applied in detection of small molecules, proteins and nucleic acids (Zhang et al., 2018; Ou et al., 2017; Lu et al., 2016; Chen et al., 2015). Taking the requirements of the simultaneous detection system for both telomerase activity and miRNAs in the complex pathological samples into consideration, the GO-based analytic strategies would make it possible for the efficient and multi-targets simultaneous detection.

Herein, we establish a telomerase and miRNA-21 (miR-21) simultaneous sensing platform with GO-based fluorescent aptasensors (GOFA). Owing to π-π stacking interaction, TS primer and telomerase/miR-21 probes would be loaded onto GO, resulting in fluorescence quenching. However, in the presence of the telomerase or miR-21, the double-stranded oligonucleotides are away from the GO surface due to the hybridization between the extended TS primers and telomerase probe as well as miR-21 and miR-21 probe, leading to obvious fluorescence recovery. We found that GOFA could simultaneously detect telomerase activity and miR-21 with low background signal, high sensitivity and simplified operation. Moreover, GOFA could be used for accurately detecting telomerase activity and miRNA in living cells and cancer patient's tissue sample. This sensing platform shows great potential in improving the accuracy in clinical diagnosis of cancer.

2. Experimental section

2.1. Materials and apparatus

RNase-free water, RNase inhibitor, deoxyribonucleotide triphosphates (dNTPs) and bull serum albumin (BSA) were purchased from TaKaRa Bio Inc. (Dalian, China). NEB buffer 2, thrombin and Bst DNA polymerase were purchased from New England Biolabs. Trypsin was purchased from Multicell Technologies. CHAPS lysis buffer was purchased from Millipore (Bedford, MA). The mirVana™ miRNA Isolation Kit was purchased from Life Technologies. GO was purchased from XFNANO Materials (Nanjing, China). All miRNAs and DNAs used in this work were synthesized by Sangon Biotech (Shanghai, China). HeLa cells and human lung fibroblast (HLF) cells were purchased from Boshide (Wuhan, China). Fresh samples from human breast cancer tissues and the corresponding non-tumor normal tissues were provided by Zhongnan Hospital (Wuhan, China). All other reagents were obtained from commercial sources without further purification. All fluorescence measurements were performed on an Agilent Cary Eclipse Fluorescence Spectrophotometer. The cell images were obtained on a Fluoview FV1200 confocal laser scanning microscope (Olympus). 3-(4,5-dimethyl-2-thiazolyl)-2,5-diphenyl-2-H-tetrazolium bromide (MTT) assay was obtained on an Infinite M200 PRO Microplate Reader (Tecan, Austria).

2.2. Cell culture

HeLa cells were cultured in 1640 medium with 10% FBS and 1% penicillin streptomycin (PS, 10,000 IU penicillin and 1000 μg/mL streptomycin, Multicell) in a culture flask at 37 °C in a humidified atmosphere containing 5% CO_2. While HLF cells were cultured in dulbecco's modified eagle medium (DMEM) under the same conditions.

2.3. Telomerase extracted from living cells and tissues samples

Cancer cells (~10^6) were collected into a clean tube, and 200 μL CHAPS lysis buffer (1 ×) was added into the tube to make a concentrate of 5000 cells/μL. After incubation with the concentrate on ice for 30 min, the mixture was centrifuged for 20 min at the max speed of 12000 × *g* at 4 °C. Then the supernatant was collected, aliquoted and stored at −80 °C.

After placing the tissue sample into a sterile mortar, liquid nitrogen was added to frozen it. And then the sample was grinded into powder with a matching pestle. The thawed sample was transferred into a sterile tube, and appropriate amount of 1 × CHAPS lysis buffer was added into this tube, then the mixture was incubated on ice for 30 min and centrifuged for 20 min at the max speed of 12000 × *g* at 4 °C. At last the supernatant was collected, aliquoted and stored at −80 °C.

2.4. The miRNAs extracted from tissues samples

The miRNAs were extracted using mirVana™ miRNA Isolation Kit according to the manufacture's protocol.

2.5. Simultaneous detection of telomerase and miRNA in solution

The experiments were performed in 50 μL solution consisting of 1 × NEB buffer, 1 mM dNTPs, 2.5 μM TS primer, 2.5 μM telomerase probes, 2.5 μM miR-21 probe, 0.5 U/μL RNase inhibitor, 25 μg/mL GO, appropriate amount of targeted telomerase and targeted miR-21. The mixtures were incubated at 37 °C for 60 min, and then transferred to 95 °C for 15 min to deactivate the telomerase. The changes of fluorescence intensity for P_{21} and P_t were recorded. The excitation (Ex) wavelength for FITC is 488, and the excitation (Ex) wavelength for Cy5 is 633.

2.6. Cytotoxicity assay

The cytotoxic potential of GO at different concentrations and incubation time was assessed with the MTT assay. HeLa cells treated with (0, 5, 10, 15, 20, 25 and 30) μg/mL GO for 12 h, 24 h, and 36 h in triplicate in a 96-well plate, respectively. The absorbance of MTT at 570 nm was recorded.

2.7. Confocal imaging of telomerase and miR-21 in living cells

When testing the platform's ability on intracellular imaging, HeLa cells were employed to be incubated with GO, TS primer, telomerase probe, or incubated with GO, miR-21 probe for 3 h under the standard cell culture conditions, respectively. As for intracellular simultaneous imaging studies, HeLa cells were incubated with GO, TS primer, telomerase probe and miR-21 probe for 3 h under the standard cell culture conditions. The control experiments with or without GO were carried out for HLF cells and HeLa cells under the same conditions. And the fluorescence images of HeLa cells were monitored by the confocal laser scanning microscope (FV1200, Olympus). The excitation (Ex) wavelength and emission (Em) wavelength for FITC are 488 and 500–550 nm, for Cy5 are 633 and 650–700 nm.

2.8. Simultaneous detection of telomerase and miRNA in tissues samples

After extracting the telomerase and miRNA from tissues samples, simultaneous detection procedure was same as it in solution.

3. Results and discussion

3.1. Design of the simultaneous detection sensing platform

As shown in Scheme 1, the proposed simultaneous detection sensing platform was composed of TS primer, Cy5-labeled telomerase probe (P_t), FITC-labeled miR-21 probe (P_{21}) and GO. The GO was serviced as an appropriate substrate for multiple probes assembling due to its large planar structure and high surface-to-volume ratio. The fluorophore-labeled P_t and P_{21} were introduced to generate multiple signals corresponding to different kinds of targets. Through π-π stacking interaction,

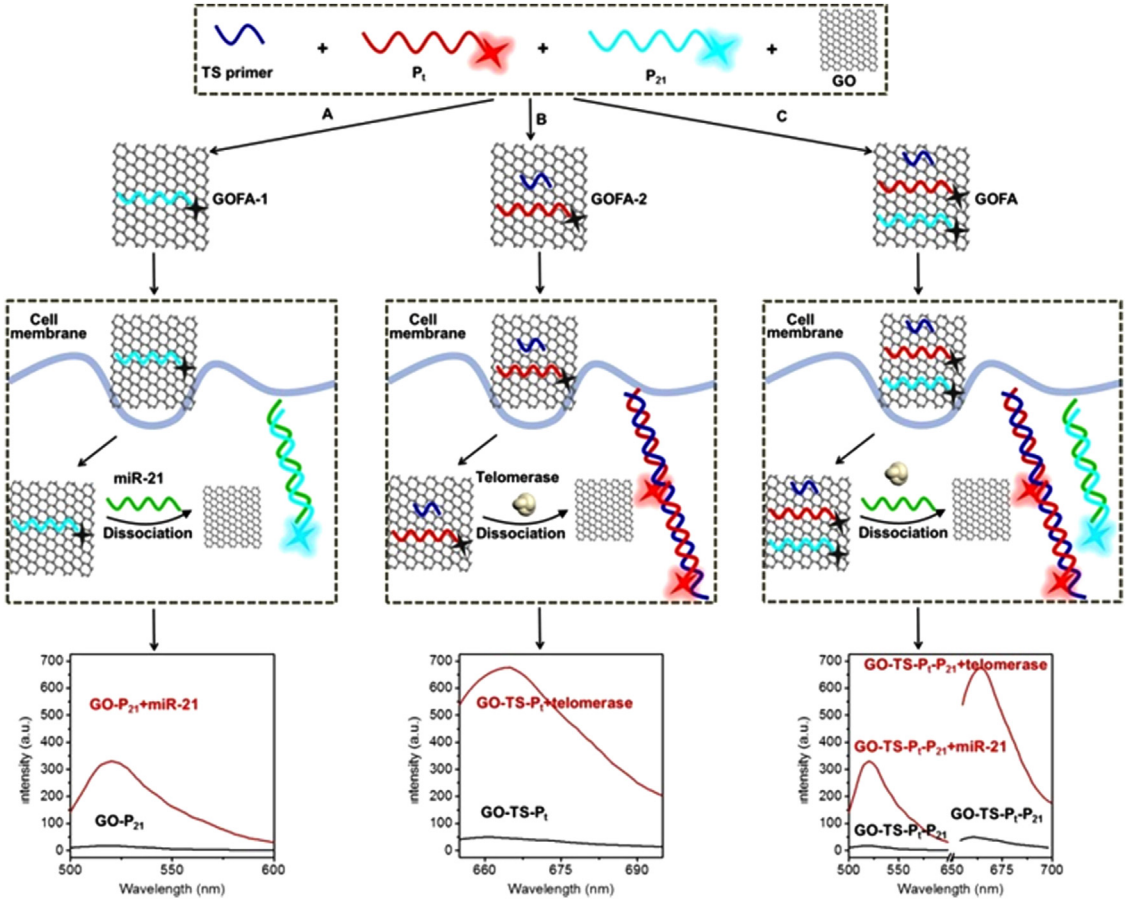

Scheme 1. Schematic illustration of the telomerase and miR-21 simultaneous detection sensing platform with GOFA-1(GO and miR-21 probe), GOFA-2 (GO, TS primer and telomerase probe) and GOFA (GO, TS primer, telomerase probe and miR-21 probe).

the ssDNAs, such as TS primer, P_t and P_{21}, could assemble onto the surface of GO and the fluorescence of dyes would be quenched by GO. It is important that a proper concentration of GO should be selected with low background signal for the sensing platform. In the presence of telomerase, the TS primer will extend as the telomeric repeat sequences (TTAGGG)n to be continuously added onto the end of the primer, forming a longer ssDNA molecule to hybridize with the P_t and form into double-stranded DNA (dsDNA) structure (Fig. S1). While for the detection of miR-21, the RNA sequence could hybridize with the P_{21} and form DNA/RNA double-stranded structure. All these double-stranded structures would far away from the GO surface because of the weak binding ability between them, leading to the fluorescence "turn on" of FITC and Cy5, respectively.

3.2. Mechanism interpretation of the sensing platform

Prior to in vitro detection of miRNA and telomerase, fluorescence quenching ability of GO was evaluated by mixing 250 nM P_{21} or P_t with different concentrations of GO from 0 to 25 μg/mL for 5 min in buffer. The fluorescence intensities of FITC and Cy5 decreased with the increased concentration of GO due to Förster resonance energy transfer (FRET) between fluorophore and GO among GOFA-1, GOFA-2 and GOFA (Fig. 1a and S2). The background signal of GOFA would be too high in the low concentration of GO, while the fluorescent recovery signal of GOFA would be restrained in the high concentration of GO. In order to get the good signal to noise ratio and make the most of experimental material, the optimized concentration of GO in GOFA was chosen as 10 μg/mL. And the quenched state of GOFA could be stabilized in PBS and serum for at least 3 h (Fig. S3).

Because of their small size and highly homologous sequences, one of the most important challenges for miRNAs detection is the specificity recognition. Thus, we have been made to optimize the miR-21 probe to improve the specificity of miRNAs detection. Based on the characteristic that GO adsorbs ssDNAs and excludes dsDNAs, the miR-21 probe was regulated through adding different numbers of Thymine (T) base to both ends of the original probe (the DNA sequence which completely complementary to the miR-21 sequence). As shown in Fig. 1b and Table S1, the original miR-21 probe could be identified by the miR-21 and released from the GO surface easily. When the number of T base increased more than 5, the miR-21 could still hybridize with miR-21 probe, but the hybridized probe could not release from the GO surface due to the strong binding interaction of long single-strand T bases. Therefore, a critical state with 3 T bases was added to both ends of the original miR-21 probe. Obviously, the specificity of miR-21 probe was enhanced, and the detecting signal from the signal base mismatch with the optimized probe (SM) was almost 4 times lower than that using the original probe (SM') (Fig. S4).

The ability of the proposed sensing platform for simultaneously detection telomerase and miR-21 was also tested. It showed that when 10 nM miR-21 and telomerase extracted from 1000 HeLa cells was coexisted in the system, the fluorescence emission peaks at 520 nm and 670 nm could be detected simultaneously (Fig. S5). These results demonstrated that the simultaneously detection of oligonucleotides and protein are easy to realize in complex environment. Control experiments were carried out by excluding GO. It was found that the fluorescence was slight changed before and after the addition of miRNA and telomerase without the help of GO (Fig. S6).

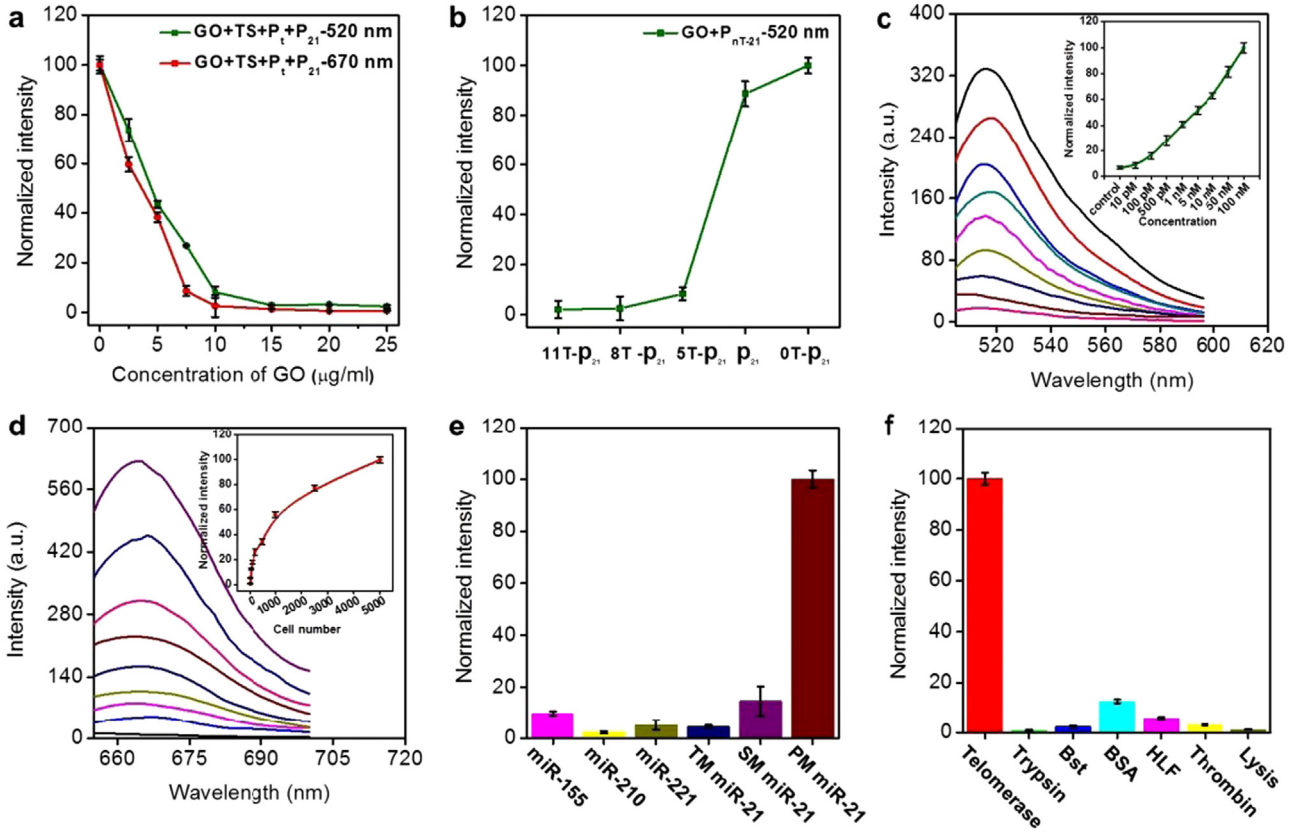

Fig. 1. (a) Normalized fluorescence intensity of 2.5 μM telo probe and 2.5 μM miR-21 probe with the concentration of GO from 0 to 25 μg/mL in reaction buffer. (b) Fluorescence emission spectra of different kinds of miR-21 probes with the same concentration of GO. (c) Fluorescence emission intensity of FITC when GOFA incubation with the different concentrations of miR-21. The inset was the relationship between fluorescence enhancement and the concentration of miR-21. (d) Fluorescence emission intensity of Cy5 when GOFA incubation with the different number of HeLa cells. The inset was the relationship between fluorescence enhancement and numbers of cancer cells. (e) Fluorescence response of the sensing system to miR-155, miR-210, miR-221, TM miR-21, SM miR-21 and PM miR-21, respectively. Concentration of all the miRNAs is 10 nM. (f) Fluorescence response of the sensing system to telomerase extracted from 1000 HeLa cells, trypsin, Bst, BSA, HLF cells, thrombin and Lysis, respectively. Concentration of the control enzymes and BSA is 5 U. Error bars were obtained from three parallel experiments.

3.3. Sensitivity of the sensing platform

To examine the sensitivity of the sensing platform, telomerase extracted from HeLa cells and synthesized miR-21 were used as the targets. To investigate the sensitivity of miR-21 detection, the fluorescence intensity was measured by adding different concentrations of miR-21. As shown in Fig. 1c and S7a, the fluorescence intensity increased with the increasing concentration of miR-21, and a detection limit of 10 pM was obtained according to the 3σ method. For telomerase analysis, it could be seen that the fluorescence intensity increased with the increasing HeLa cell numbers in the range of 0–5000 cells (Fig. 1d). The mean value of the controls adds 3 times of the standard deviation was set as the threshold line (i. e. the 3σ method). The detection limit was estimated to be equivalent to 10 HeLa cells (Fig. S7b).

3.4. Selectivity of the sensing platform

In order to evaluate its selectivity, miR-155, miR-210, miR-221, single-base mismatched miR-21 (SM miR-21) and three-base mismatched miR-21 (TM miR-21) were applied as the negative controls when detecting miR-21 target (Table S1). Results shown that the signal from the perfectly matched miR-21 (PM miR-21) can be discriminated from others obviously (Fig. 1e). To investigate the specificity of the sensing platform for telomerase detection, negative controls such as trypsin, Bst DNA polymerase (Bst), BSA, telomerase extracted from 1000 HLF cells, thrombin and lysis buffer (Lysis) were used. The results showed in Fig. 1f confirmed that there would no process of extension on the TS primer if no telomerases were contained in the solution.

3.5. Determination of telomerase and miR-21 in living cells

As GO shows good biocompatibility, considerable intracellular transport capacity, and efficient protection for nucleic acids from enzymatic cleavage, this sensing platform could be applied to detect tumor markers in living cells. Firstly, the cytotoxicity of GO to HeLa cells was evaluated. GO exhibited relatively low cytotoxicity to HeLa cells at different concentrations (< 30 μg/mL) and in the limited time range (< 36 h) (Fig. S8). For intracellular imaging studies, 10 μg/mL of GOFA were chosen and incubated with cells for 3 h. Only one kind of fluorescence signal derived from P_{21} or P_t was clearly observed after incubation with GOFA-1 and GOFA-2, respectively (Fig. 2a and b). In the simultaneous intracellular imaging studies, both of the fluorescence signals derived from P_{21} and P_t were distinctly observed after incubation with GOFA (Fig. 2c). The faint fluorescence signals were observed in the normal cells (HLF cells) after incubation with GOFA and the naked fluorescent aptasensor (Fig. 2d and S9). The 3D surface projections of Z-stack images for GOFA incubation with HeLa cells further confirmed this result (Fig. 2e).

3.6. Determination of telomerase and miRNA in tissues samples

Since the expression levels of certain miRNAs as well as the activity of telomerase are accurate predictors of the patient's overall prognosis, the expression levels of miRNAs and telomerase extracted from breast cancer patient tissues samples and healthy people tissues samples were assayed to appreciate whether this platform possess the applicability for clinical diagnosis. Crude extracts from six breast cancer patient tissues

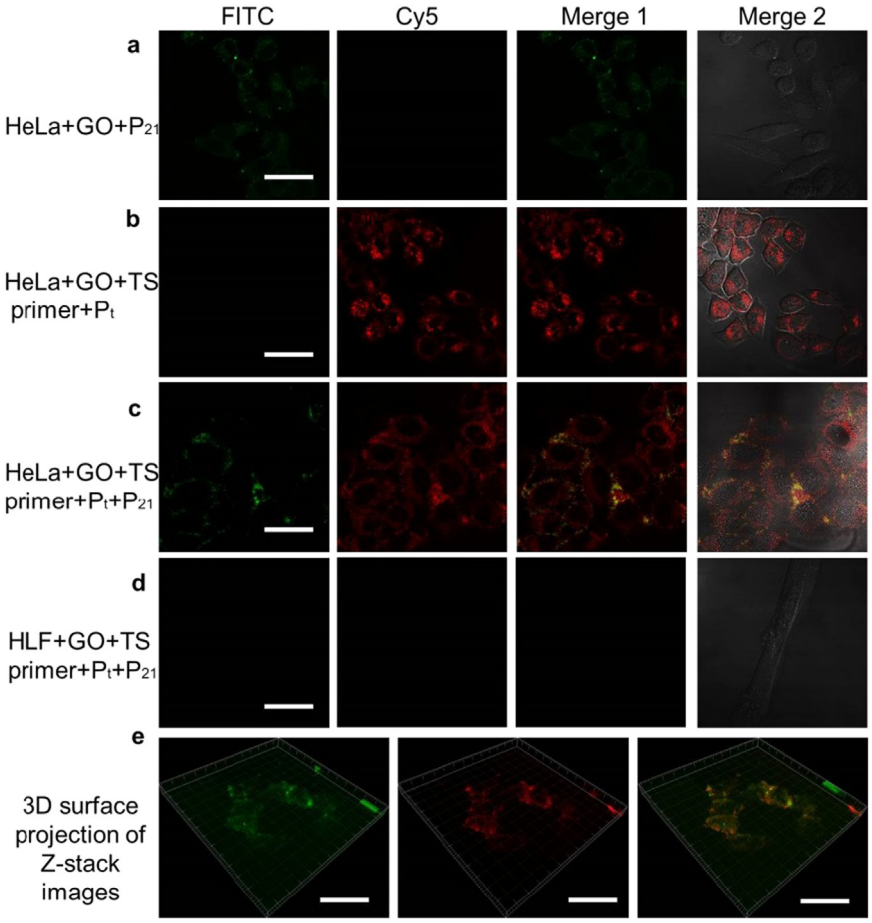

Fig. 2. Confocal images of telomerase activity and miR-21 in living cells. HeLa cells were treated with (a) GOFA-1; (b) GOFA-2; (c) GOFA respectively. And (d) HLF cells were treated with GOFA. Scale bar was 50 μm. (e) The 3D surface projection of Z-stack images for HeLa cells treated with GOFA. Scale bar was 20 μm.

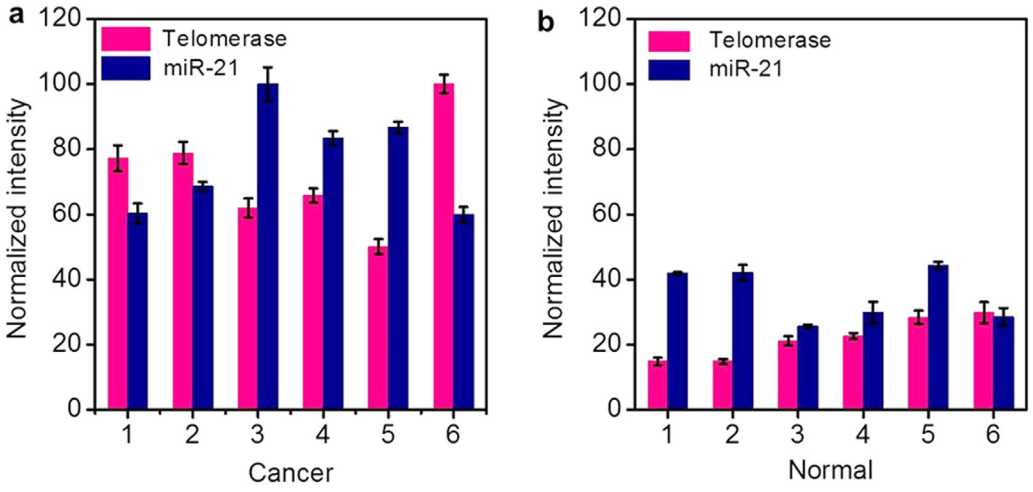

Fig. 3. The fluorescent intensity of GOFA from telomerase and miR-21 detection with the addition of cancer patient tissue samples (a) and normal people tissue samples (b). Error bars were obtained from three parallel experiments.

samples and six healthy people tissues samples were performed in this study. As shown in Fig. 3, all the detected signal intensities corresponding to the telomerase activity and miR-21 concentration from the cancer samples were significantly higher than that of the normal samples. These results demonstrated that this sensing platform holds great promise for cancer diagnosis with excellent selectivity and accuracy.

4. Conclusions

In conclusion, a sensing platform GOFA for the simultaneous detection of telomerase and miR-21 based on GO, TS primer and fluorophore-labeled telomerase/miR-21 oligonucleotide has been developed. It validated to simultaneously detect telomerase activity and miR-21 with high stability, sensitivity and selectivity that the detection limit determined was 10 pM and 10 HeLa cells. Subsequently, GOFA showed

remarkable image effect in HeLa cells than that in HLF cells. Moreover, it further verified that GOFA could distinguish telomerase and miR-21 between cancer patient tissue samples and normal people tissue samples. Due to its low background signal, simplified operation, high sensitivity and selectivity, GOFA could offer more comprehensive and reliable information and show great potential in improving the accuracy in clinical diagnosis of cancer. We anticipate that GOFA will provide new opportunities for further understanding the relationship between telomerase activity, miRNA and cancer in personalized medicine.

Acknowledgments

This work is supported by the National Basic Research Program of China (973 Program, 2015CB932600) , the National Key R&D Program of China (2017YFA0208000, 2016YFF0100800) , the National Natural Science Foundation of China (21525523, 21722507, 21574048, 21874121), The Fok Ying-Tong Education Foundation, China (151011), China Postdoctoral Science Foundation funded project (2017M620309, 2017M622402). We thank Dr. Fubing Wang and Changqing Yin in Zhongnan Hospital (Wuhan, China) to provide the human breast cancer tissue samples and the normal tissue samples.

Appendix A. Supporting information

Supplementary data associated with this article can be found in the online version at doi:10.1016/j.bios.2018.10.009.

References

Agasti, S.S., Rana, S., Park, M., Kim, C.K., You, C., Rotello, V.M., 2010. Adv. Drug. Deliv. Rev. 62, 316–328.
Blasco, M.A., 2005. Nat. Rev. Genet. 6, 611–622.
Chen, Y., Tan, C., Zhang, H., Wang, L., 2015. Chem. Soc. Rev. 44, 2681–2701.
Cheng, Y., Dai, J., Sun, C., Liu, R., Zhai, T., Lou, X., Xia, F., 2018. Angew. Chem. Int. Ed. 57, 3123–3127.
Croce, C.M., 2009. Nat. Rev. Genet. 10, 704–714.
Du, Y., Li, B., Wang, E., 2012. Acc. Chem. Res. 46, 203–213.
Duan, R., Zuo, X., Wang, S., Quan, X., Chen, D., Chen, Z., Jiang, L., Fan, C., Xia, F., 2013. J. Am. Chem. Soc. 135, 4604–4607.
Etzioni, R., Urban, N., Ramsey, S., McIntosh, M., Schwartz, S., Reid, B., Radich, J., Anderson, G., Hartwell, L., 2003. Nat. Rev. Cancer 3, 243–252.
Li, N., Chang, C., Pan, W., Tang, B., 2012. Angew. Chem. Int. Ed. 51, 7426–7430.
Liu, F., Choi, J.Y., Seo, T.S., 2010. Biosens. Bioelectron. 25, 2361–2365.
Loh, K.P., Bao, Q., Eda, G., Chhowalla, M., 2010. Nat. Chem. 2, 1015–1024.
Long, Z., Zhan, S., Gao, P., Wang, Y., Lou, X., Xia, F., 2018. Anal. Chem. 90, 577–588.
Lou, X., Zhuang, Y., Zuo, X., Jia, Y., Hong, Y., Min, X., Zhang, Z., Xu, X., Liu, N., Xia, F., Tang, B.Z., 2015. Anal. Chem. 87, 6822–6827.
Lu, C., Jimmy Huang, P., Ying, Y., Liu, J., 2016. Biosens. Bioelectron. 79, 244–250.
Ou, X., Hong, F., Zhang, Z., Cheng, Y., Zhao, Z., Gao, P., Lou, X., Xia, F., Wang, S., 2017. Biosens. Bioelectron. 89, 417–421.
Pan, W., Liu, B., Gao, X., Yu, Z., Liu, X., Li, N., Tang, B., 2018. Nanoscale 10, 14264–14271.
Pan, W., Zhang, T., Yang, H., Diao, W., Li, N., Tang, B., 2013. Anal. Chem. 85, 10581–10588.
Pei, H., Li, J., Lv, M., Wang, J., Gao, J., Lu, J., Li, Y., Huang, Q., Hu, J., Fan, C., 2012. J. Am. Chem. Soc. 134, 13843–13849.
Qian, R., Ding, L., Yan, L., Lin, M., Ju, H., 2014. J. Am. Chem. Soc. 136, 8205–8208.
Wang, X., Dai, J., Min, X., Yu, Z., Cheng, Y., Huang, K., Yang, J., Yi, X., Lou, X., Xia, F., 2018. Anal. Chem. 90, 8162–8169.
Wang, Y., Li, Z., Weber, T.J., Hu, D., Lin, C., Li, J., Lin, Y., 2013. Anal. Chem. 85, 6775–6782.
Wei, B., Zhai, Z., Wang, H., Zhang, J., Xu, C., Xu, Y., He, L., Xie, D., 2018. J. Agric. Food Chem. 66, 9080–9086.
Wu, L., Qu, X., 2015. Chem. Soc. Rev. 44, 2963–2997.
Yang, L., Li, J., Pan, W., Wang, H., Li, N., Tang, B., 2018. Chem. Commun. 54, 3656–3659.
Zang, Z., Zeng, X., Wang, M., Hu, W., Liu, C., Tang, X., 2017a. Sens. Actuators B-Chem. 252, 1179–1186.
Zhang, H., Zhang, H., Aldalbahi, A., Zuo, X., Fan, C., Mi, X., 2017b. Biosens. Bioelectron. 89, 96–106.
Zhang, L., Peng, J., Hong, M.F., Chen, J.Q., Liang, R.P., Qiu, J.D., 2018. Analyst 143, 2334–2341.
Zhang, X., Lou, X., Xia, F., 2017c. Theranostics 2017 (7), 1847–1862.
Zhao, Y., Chen, F., Li, Q., Wang, L., Fan, C., 2015. Chem. Rev. 115, 12491–12545.
Zhou, X., Xing, D., 2012. Chem. Soc. Rev. 41, 4643–4656.